

Self-doped Molecular Mott Insulator for Bilayer High-Temperature Superconducting $\text{La}_3\text{Ni}_2\text{O}_7$

Zhan Wang,^{1,2} Kun Jiang,^{3,4,*} and Fu-Chun Zhang^{2,5,†}

¹Department of Physics, Boston College, Chestnut Hill, Massachusetts 02467, USA

²Kavli Institute for Theoretical Sciences, University of Chinese Academy of Sciences, Beijing, 100190, China

³Beijing National Laboratory for Condensed Matter Physics and Institute of Physics, Chinese Academy of Sciences, Beijing 100190, China

⁴School of Physical Sciences, University of Chinese Academy of Sciences, Beijing 100190, China

⁵Collaborative Innovation Center of Advanced Microstructures, Nanjing University, Nanjing 210093, China

(Dated: January 13, 2025)

The bilayer structure of recently discovered high-temperature superconducting nickelates $\text{La}_3\text{Ni}_2\text{O}_7$ provides a new platform for investigating correlation and superconductivity. Starting from a bilayer Hubbard model, we show that there is a molecular Mott insulator limit forming by the bonding band owing to Hubbard interaction and large interlayer coupling. This molecular Mott insulator becomes self-doped from electrons transferred to the antibonding bands at a weaker interlayer coupling strength. The self-doped molecular Mott insulator is similar to the doped Mott insulator studied in cuprates. We propose $\text{La}_3\text{Ni}_2\text{O}_7$ is a self-doped molecular Mott insulator, whose molecular Mott limit is formed by two nearly degenerate antisymmetric $d_{x^2-y^2}$ and d_{z^2} orbitals. Partial occupation of higher energy symmetric $d_{x^2-y^2}$ orbital leads to self-doping, which may be responsible for high-temperature superconductivity in $\text{La}_3\text{Ni}_2\text{O}_7$.

The discovery of high-temperature superconductivity (SC) in cuprates greatly challenges our understanding of condensed matter physics [1]. The underlying physics of cuprates is widely believed to be deeply related to electron correlation and their parent Mott insulator states [2, 3]. Hence, doping a Mott insulator is one central role for realizing a high-temperature superconductor. Following this idea, it was proposed that doping the Mott nickelates could also lead to high-temperature superconductivity [4]. This idea became realized in thin films of the “infinite-layer” nickelates $(\text{Sr},\text{Nd})\text{NiO}_2$ in 2019 [5–7], which opened the Nickel age of superconductivity [8]. Recently, a new type of nickelates $\text{La}_3\text{Ni}_2\text{O}_7$ (LNO) was successfully synthesized with a high-temperature superconducting transition $T_c \sim 80\text{K}$ under high pressure [9–14]. Many theoretical proposals have been developed to uncover its superconducting mechanism [15–31].

Compared to the essential CuO_2 layer in cuprates, the central ingredient for $\text{La}_3\text{Ni}_2\text{O}_7$ is the bilayer NiO structure. The valence charge of Ni is $3d^{7.5}$, away from any strongly correlation limit. Hence, the bilayer structure is inseparable and what is their Mott limit becomes one important question. Theoretically, the bilayer systems have been explored many years ago, especially the bilayer Hubbard model [32–39]. In this work, we want to show that the correlation parent limit of this bilayer structure is the molecular Mott insulator, and self-doping this Mott insulator leads to the high-temperature superconductivity.

In the non-interacting limit, the bilayer coupling energy η separates the bilayer bands into bonding and anti-bonding bands as illustrated in Fig.1 (a1, b1). Notice that the Wannier orbitals for bonding and anti-bonding bands are linear combinations of atomic orbitals in different layers. Hence, these Wannier orbitals should be considered as *molecular orbitals*. Taking Hubbard’s interaction into account, this η competes with U and the bandwidth, leading to different insulating limits beyond the upper and lower Hubbard bands in the single-band Hubbard model.

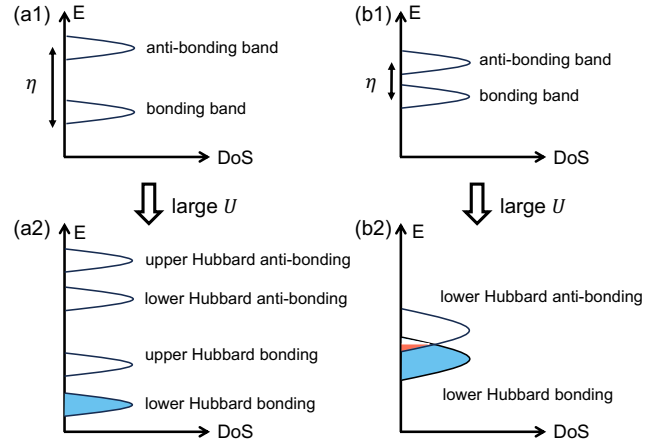


FIG. 1. Self-doped Molecular Mott insulator. (a1) and (b1) show bands formed by molecular bonding and anti-bonding orbitals that are associated with large and small molecule orbital splitting η , respectively. (a2) and (b2) show the Hubbard band resulting from on-site repulsion U . Consider one electron per molecule, in the scenario of (a2) where η is large compared to the band width, the four Hubbard bands are isolated from each other and the electrons will fill the lower bonding Hubbard band only. In the scenario of (b2) where η is relatively small, there is finite overlap between the lower Hubbard bands of the molecular orbitals. The electrons now resides primarily in the lower bonding Hubbard band, with a small portion in the lower anti-bonding Hubbard band, giving rise to the self-doped molecular Mott insulator.

There are two typical scenarios depending on η , as schematically illustrated in Fig.1. In the first case where η is large, the four Hubbard bands are well separated from each other. Here, considering quarter filling, we get the singly occupied lower Hubbard bonding band. The effective theory for this case in terms of molecular orbitals shares the same feature of the single-band Mott insulator. Therefore, it is a *molecular Mott insulator*. A much intriguing scenario is expected when the molecular energy splitting decreases, as shown in Fig.1

(b). In this case, the two lower Hubbard bands of the bonding and anti-bonding orbitals overlap. The lower bonding Hubbard band becomes hole-doped due to the overlap, which we call the self-doped molecular Mott insulator.

As a concrete model to realize the self-doped molecular Mott insulator, consider the bilayer square lattice Hubbard model as shown in Fig.2 (a). The Hamiltonian can be written as:

$$H = H_t + H_U. \quad (1)$$

with the kinetic part H_t and the interaction part H_U given by:

$$H_t = -t \sum_{\langle ij \rangle, \sigma} \sum_{l=t,b} c_{i l \sigma}^\dagger c_{j l \sigma} - \frac{\eta}{2} \sum_{i, \sigma} c_{i t \sigma}^\dagger c_{i b \sigma} + \text{h.c.} \quad (2)$$

$$H_U = U \sum_i \sum_{l=t,b} n_{i l \uparrow} n_{i l \downarrow}. \quad (3)$$

Here $l = t, b$ is the layer index for the top and the bottom layer, respectively. $c_{i l \sigma}^\dagger$ creates an electron with spin σ at site i of layer l and $n_{i l \sigma}$ is the corresponding electron number operator. The two layers have the same in-plane nearest neighbor hopping amplitudes t and the repulsive Hubbard interaction U . The interlayer hopping is denoted as $\frac{\eta}{2}$.

The kinetic part can be diagonalized to yield the interlayer molecular bonding (+) and anti-bonding (-) orbitals, namely $c_{i \pm \sigma} = (c_{i t \sigma} \pm c_{i b \sigma}) / \sqrt{2}$ as labeled by blue and red in Fig.2 (a). The associated molecular energy dispersions are given by $E_{\pm} = \epsilon_k \mp \frac{\eta}{2}$. The molecular energy splitting is given by the interlayer hopping amplitude, which is depicted in Fig.2 (b) for $\eta > 0$. The band width is determined by the in-plane hopping t and the band energy splitting corresponds to η . For $\frac{\eta}{2} \leq 2t$, we find there is always an overlap between the bonding and the anti-bonding bands. In this case, with strong Hubbard U , it is expected the local electrons are mostly found in the lower bonding Hubbard band, with a small number of electrons in the anti-bonding Hubbard band, similar to the scenario depicted in Fig.1 (b).

It is well known that the doped Mott insulator can be well described by the effective t - J model [2, 3, 40]. For this self-doped molecular Mott insulator, we can also write down an effective t - J model. Compared to the single band t - J model, there are four possible energy-allowed states: hole, singly-occupied $|-\rangle_\sigma$, singly-occupied $|+\rangle_\sigma$ and a special doublon state $|+\rangle_\sigma \otimes |-\rangle_\sigma$, as summarised in Fig.2 (c). This doublon state is formed by occupying both the bonding and the anti-bonding orbitals of the same spin. The configuration is found to be immune from double occupancy constraints. One can see this through its wavefunction:

$$\begin{aligned} c_{i+\sigma}^\dagger \otimes c_{i-\sigma}^\dagger &= \frac{1}{\sqrt{2}}(c_{i t \sigma}^\dagger + c_{i b \sigma}^\dagger) \otimes \frac{1}{\sqrt{2}}(c_{i t \sigma}^\dagger - c_{i b \sigma}^\dagger) \\ &= c_{i t \sigma}^\dagger \otimes c_{i b \sigma}^\dagger. \end{aligned} \quad (4)$$

Hence this doublon state corresponds to filling one electron at each layer and doesn't cost U . With total electron number

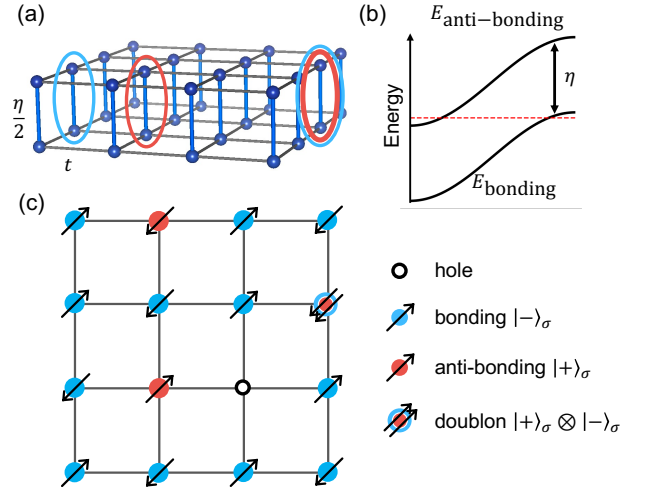


FIG. 2. Self-doped molecular Mott insulator from the bilayer Hubbard model. (a) schematic illustration of the bilayer Hubbard model. The interlayer hopping is written as $\frac{\eta}{2}$ and the intralayer hopping as t . With η dominant, the top and bottom layer forms molecular bonding and anti-bonding orbitals circled by blue and red, respectively. (b) Energy dispersion of the bonding and the anti-bonding molecular orbitals. With $\frac{\eta}{2} < 2t$, the ground state with one electron per molecule contains both the bonding and anti-bonding orbitals. (c) Schematic illustration of the self-doped molecular Mott insulator with large Hubbard U . The blue and red circles denote the electrons in the bonding and the anti-bonding orbitals, respectively. Note the depicted doublon state with both orbitals occupied doesn't cost U and is also allowed in the low energy range.

of one per site, the formation of a doublon will also generate a hole on another site, as shown in Fig.2 (c). Therefore, the effective t - J model can be written down as

$$H_{t-J} = -t_+ \sum_{\langle ij \rangle, \sigma} \hat{P}_G (c_{i+\sigma}^\dagger c_{j+\sigma} + \text{h.c.}) \hat{P}_G + J \sum_{\langle ij \rangle} \mathbf{S}_{i+} \cdot \mathbf{S}_{j+} \quad (5)$$

Here $\mathbf{S}_{i+} = \frac{1}{2} c_{i+\sigma}^\dagger \boldsymbol{\sigma}_{\alpha\beta} c_{i+\sigma}$ denotes the local spin operator of the bonding electron. \hat{P}_G is the projection operator to the above energy-allowed configurations. Since the correlation effect in anti-bonding orbitals is weak, we only treat them as self-doping to the bonding t - J model. Owing to self-doping, the t - J model can naturally induce a d -wave superconductivity, as widely studied in cuprates [2, 3, 41].

Furthermore, we want to demonstrate that $\text{La}_3\text{Ni}_2\text{O}_7$ is a concrete realization of the self-doped molecular Mott insulator. The crystal structure of the $\text{La}_3\text{Ni}_2\text{O}_7$ material under high pressure has the space group $Fmmm$, with stacked bilayer NiO_2 planes formed by corner-sharing Ni-O octahedra along the apical direction. Due to the octahedra crystal field and Jahn-Teller distortion, the partially-filled e_g orbitals form the atomic occupancy of bilayer $\text{Ni}^{2.5+}$ atoms, as illustrated in Fig.3 (a). Taking the interlayer coupling into account, the molecular orbitals for e_g orbitals are further split into four energy levels in Fig.3 (a).

Notice that owing to the different symmetry properties of

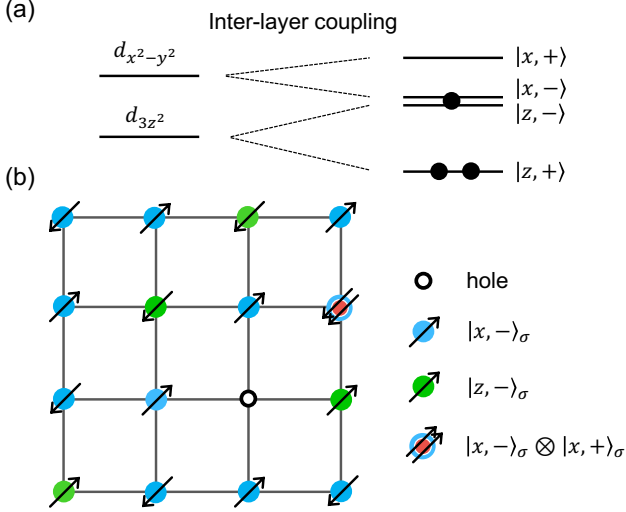


FIG. 3. Model for $\text{La}_3\text{Ni}_2\text{O}_7$: two-orbital self-doped Molecular Mott insulator. (a) Local electronic orbitals of the interlayer pair $(2\text{Ni})^{5+}$. For each Ni atom, the e_g orbitals possess higher atomic energy due to crystal field splitting. With interlayer coupling $t_{\perp}^{x,z}$, the two sets of e_g orbitals further split into four molecular orbitals. Two electrons occupy the $|z, +\rangle$ orbital which is well lower in energy than the other three orbitals. The remaining electron predominantly occupies one of the two anti-bonding orbitals $|x, -\rangle_{\sigma}$ and $|z, -\rangle_{\sigma}$, with a small portion in the bonding orbital $|x, +\rangle_{\sigma}$. (b) Schematic illustration of the self-doped Molecular Mott insulator. In the Mott limit, electrons can only occupy either one of the $|x, -\rangle_{\sigma}$ and $|z, -\rangle_{\sigma}$ orbitals due to the strong onsite Hubbard repulsion, as depicted in blue and green, respectively. A small amount of doublon states, namely $|x, -\rangle_{\sigma} \otimes |x, +\rangle_{\sigma}$ as depicted in blue-red circles, can exist due to no cost in U. With the total number of electrons fixed, formation of a doublon will generate a hole, leading to the self-doped Molecular Mott insulator.

d_{z^2} orbital and $d_{x^2-y^2}$ orbital along z -direction, the molecular energy splittings induced by the interlayer hopping $t_{\perp}^{x,z}$ are opposite for the two orbitals. The molecular bonding orbital of the d_{z^2} , denoted as $|z, +\rangle$, has much lower energy and is fully occupied. We therefore drop this orbital in the following discussion. It is interesting that the Jahn-Teller distortion is comparable with $t_{\perp}^{x,z}$ in $\text{La}_3\text{Ni}_2\text{O}_7$ [42]. This leads to a nearly degenerate antisymmetric e_g orbitals denoted as $|x, -\rangle$ and $|z, -\rangle$. And the symmetric $|x, +\rangle$ is slightly higher than these antisymmetric e_g orbitals. Therefore, the one-electron-filled antisymmetric e_g orbitals form a molecular Mott insulator. Self-doping this molecular Mott insulator owing to $|x, +\rangle$ gives us the physics of $\text{La}_3\text{Ni}_2\text{O}_7$.

More precisely, the effective Hamiltonian for $\text{La}_3\text{Ni}_2\text{O}_7$ contains 3 parts: $H = H_1 + H_2 + H_{12}$. For $|x, +\rangle_{\sigma}$, the Hamil-

tonian reads:

$$H_1 = - \sum_{\langle ij \rangle, \sigma} t_{ij}^{\dagger} (f_{ix\sigma}^{\dagger} f_{jx\sigma} + \text{h.c.}) + \epsilon_{x+} \sum_{i\sigma} f_{ix\sigma}^{\dagger} f_{ix\sigma}, \quad (6)$$

where $f_{ix\sigma}^{\dagger}$ is the creation operator corresponding to $|x, +\rangle_{\sigma}$ with spin σ and $\epsilon_{x+} > 0$ denotes the molecular energy shift of the bonding orbital. For the two degenerate antisymmetric orbitals $|x, -\rangle_{\sigma}$ and $|z, -\rangle_{\sigma}$,

$$H_2 = - \sum_{\langle ij \rangle, \alpha\alpha', \sigma} t_{ij}^{\alpha\alpha'} (c_{i\alpha\sigma}^{\dagger} c_{j\alpha'\sigma} + \text{h.c.}) + \sum_{i\alpha} U^{\alpha\alpha} n_{i\alpha\uparrow} n_{i\alpha\downarrow} + \sum_{i\alpha} U^{\alpha\bar{\alpha}} (n_{i\alpha\uparrow} + n_{i\alpha\downarrow})(n_{i\bar{\alpha}\uparrow} + n_{i\bar{\alpha}\downarrow}). \quad (7)$$

Here $c_{i\alpha\sigma}^{\dagger}$ with $\alpha = x, z$ is the creation operator associated with $|x, -\rangle_{\sigma}$ and $|z, -\rangle_{\sigma}$ and $n_{i\alpha\sigma}$ is the electron number operator. The in-plane hopping amplitude is denoted as $t_{ij}^{\alpha\alpha'}$, and the inter- and intra-orbital Hubbard interactions is denoted as $U^{\alpha\alpha'}$. H_{12} denotes their coupling, which doesn't contain pair hopping term due to symmetry constraint.

In the large $U^{\alpha\alpha'}$ limit, the Hamiltonian H_2 alone defines a molecular Mott insulator at one-electron filling with nearly orbital degeneracy [43–45]. This e_g orbital degenerate Mott insulator has been discussed with equal importance of spin and orbital degrees of freedom [43–45]. In real materials, the molecular energy cost ϵ_{x+} is small. Introducing a small number of $|x, +\rangle_{\sigma}$ will cost molecular energy but gain kinetic energy. Similar to the second scenario mentioned in the bilayer Hubbard model, with small number of $|x, +\rangle_{\sigma}$ generated, one gets the doublon state $|x, -\rangle_{\sigma} \otimes |x, +\rangle_{\sigma}$ as well as self-doped holes, as depicted in Fig.3 (b). It is essential to elucidate the correlation effect of different types of particles in the self-doped molecular Mott insulator. With one electron per site, the $|x, -\rangle_{\sigma}$ and $|z, -\rangle_{\sigma}$ at site i can only move to neighboring empty sites, which is of density $\sim n_{x+}/2 \ll 1$, and therefore are highly correlated. The bonding electron $|x, +\rangle_{\sigma}$ at site i may move to neighbor $|x, -\rangle_{\sigma}$ with density $\sim n_{x-}/2 \sim 1/2$ and is therefore weakly correlated. We expect the superconductivity is primarily induced by the $|x, -\rangle_{\sigma}$ and $|z, -\rangle_{\sigma}$ electrons.

The low-energy effective Hamiltonian in the large- U limit can be derived following the work by Castellani et al[44]. Because the bonding orbitals $|x, +\rangle_{\sigma}$ are weakly correlated, its effects can be well approximated by doping additional holes into the system described by H_2 . We neglect the Hund's coupling term here in the interorbital Hubbard term, leading to $U^{xz} = U^{xx} = U^{zz} = U$. The effective interaction part of the Hamiltonian derived from H_2 can be written as:

$$H_{int} = -\frac{1}{U} \sum_{\langle ij \rangle} \sum_{\alpha\alpha'\beta} \sum_{\sigma} t_{ij}^{\alpha\beta} t_{ij}^{\alpha'\beta} (c_{i\alpha\sigma}^{\dagger} c_{i\alpha'\sigma} c_{j\beta\bar{\sigma}}^{\dagger} c_{j\beta\sigma} - c_{i\alpha\sigma}^{\dagger} c_{i\alpha'\bar{\sigma}} c_{j\beta\bar{\sigma}}^{\dagger} c_{j\beta\sigma} + c_{i\alpha\sigma}^{\dagger} c_{i\alpha'\sigma} c_{j\beta\bar{\sigma}}^{\dagger} c_{j\beta\bar{\sigma}} + c_{i\alpha\sigma}^{\dagger} c_{i\alpha'\sigma} c_{j\beta\sigma}^{\dagger} c_{j\beta\sigma}) - t_{ij}^{\alpha\beta} t_{ij}^{\alpha'\bar{\beta}} (c_{i\alpha\sigma}^{\dagger} c_{i\alpha'\bar{\sigma}} c_{j\beta\bar{\sigma}}^{\dagger} c_{j\beta\sigma} + c_{i\alpha\sigma}^{\dagger} c_{i\alpha'\sigma} c_{j\beta\bar{\sigma}}^{\dagger} c_{j\beta\sigma}). \quad (8)$$

Here the orbital index $\alpha\alpha'\beta$ can take either x or z , referring to the two antisymmetric orbitals $|x, -\rangle$ and $|z, -\rangle$. The inverse index, e.g β , refers to the other orbital with the different index from α . This Hamiltonian is another version of Kugel-Khomskii (KK) Hamiltonian [43]. The hopping part is given by:

$$H_0 = - \sum_{\langle ij \rangle, \alpha\alpha'} t_{ij}^{\alpha\alpha'} \hat{P}_G (c_{i\alpha\sigma}^\dagger c_{j\alpha'\sigma} + \text{h.c.}) \hat{P}_G. \quad (9)$$

Here \hat{P}_G denotes the projection onto the above Hilbert space in the large- U limit. The hopping parameter $t_{ij}^{\alpha\alpha'}$ can be obtained from first-principle calculations [27].

The superconducting pairing symmetry is analyzed using the renormalized mean field theory [41]. The effective Hamiltonian of the self-doped molecular Mott insulator is given by:

$$H = H_0 + H_1 + H_{int}, \quad (10)$$

where we set t_{ij}^+ in H_1 equals t_{ij}^{xx} in H_0 . The number of self-doped holes n_h , coming from the electrons from the $|x, +\rangle$ orbital, is controlled by ϵ_{x+} in H_1 with $n_h = n_{x+}$. To account for the double occupancy constraint imposed by \hat{P}_G in H_0 , we introduce the Gutzwiller factor $g_t^{\alpha\alpha'} = \frac{2n_h}{\sqrt{(2-n_\alpha)(2-n_{\alpha'})}}$ [46, 47], where n_h denotes the number of self-doped holes, and n_α is the total electron number from the orbital $\alpha \in \{x, z\}$.

The pairing mean field in the singlet channel is defined as:

$$\Delta_{ij}^{\alpha\alpha'} = \langle c_{i\alpha\uparrow}^\dagger c_{j\alpha'\downarrow}^\dagger \rangle - \langle c_{i\alpha\downarrow}^\dagger c_{j\alpha'\uparrow}^\dagger \rangle. \quad (11)$$

with $\alpha, \alpha' \in \{x, z\}$, containing contributions from both the inter- and intra-orbital pairs. The mean field Hamiltonian and the self-consistent equations are derived in the supplementary material. In comparison to the single orbital $t - J$ model, there are two types of pairing order parameters: the intra-orbital pairing Δ^{xx} , Δ^{zz} and the interorbital pairing Δ^{xz} , and their competition leads to different pairing symmetries.

The parameters in the calculations are chosen as follows. The Hubbard interaction $U = 6$ and the nearest neighbor hoppings are set as $t^{xx} = 1$, $t^{zz} = 0.2$. As for interorbital hoppings, we consider two cases with $t^{xz} = 0.1$ and $t^{xz} = 0.8$. The calculations are performed as a function of self-doped hole density n_h . Each n_h corresponds to a specific ϵ_{x+} , e.g $n_h = 0.1$ can be obtained with $\epsilon_{x+} \approx 3$. The pairing symmetry can be categorized according to the representation of the lattice symmetry group D_{4h} . In the singlet channel, pairing between the nearest neighbors can belong to either the extended s -wave (A_{1g} representation), denoted as Δ_s , with the same sign in the x and y directions, or the d -wave (B_{1g} representation), denoted as Δ_d , with alternating signs. The mean field results are plotted in Fig.4. For $t_{xz} = 0.1$, as shown in Fig.4 (a), we find the pairing symmetry follows d -wave, similar to the single orbital $t - J$ model. In this case, the pairings are found to be dominated by Δ^{xx} (red solid line), i.e the intra-orbital process from $|x, -\rangle$ orbital. Δ^{xz} (green dash-dot line) is found to be significantly smaller due to small t^{xz} . Δ^{zz} is also small due to small particle

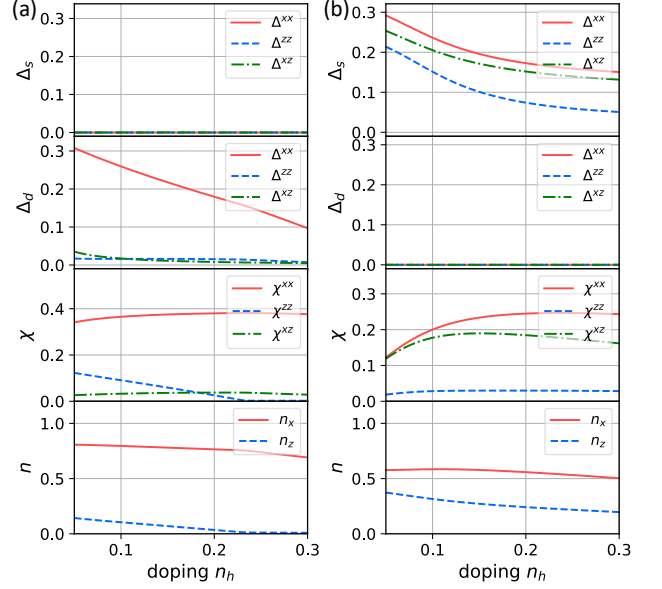


FIG. 4. Mean field results for the two-orbital self-doped molecular Mott insulator obtained with in-plane intra-orbital hopping $t^{xx} = 1$, $t^{zz} = 0.2$, and inter-orbital hopping $t^{xz} = 0.1$ (a), $t^{xz} = 0.8$ (b), plotted as a function of the self-doped hole density n_h . The Hubbard interaction is set as $U = 6$. The figures from top to bottom show the results for the pairing component from extended s -wave Δ_s , d -wave Δ_d , the hopping mean field χ and the occupation number $n_{x,z}$. With increasing interorbital hybridization t^{xz} , we find the pairing symmetry changes from d -wave to s -wave.

number n_z , as shown in the lowest panel. For $t^{xz} = 0.8$, as shown in Fig.4 (b), the pairing solution is found to agree with the extended s -wave. In this case, both intra- and interorbital pairings are of similar magnitudes, suggesting strong interorbital effects. Moreover, the electron occupation number difference $n_x - n_z$ becomes much smaller as the interorbital hopping increases from $t^{xz} = 0.1$ to $t^{xz} = 0.8$, which also points to the enhanced inter-orbital effects. We therefore conclude based on the above calculations that the extended s -wave pairing can be favored due to significant interorbital effect. For intermediate t^{xz} , the competition between s - and d -wave instability can induce more interesting pairing solutions and requires further study.

In this paper, we start with two e_g orbitals ($d_{x^2-y^2}$ and d_{z^2}) for double layer $\text{La}_3\text{Ni}_2\text{O}_7$. We consider inter-layer coupling for d_{z^2} orbitals to be strong and the two Ni-sites in the top and bottom layers form a molecule. The bonding states of d_{z^2} are all occupied leaving one e_g electron per molecule on average for the anti-bonding d_{z^2} and both bonding and anti-bonding states of $d_{x^2-y^2}$. In the large on-site of Coulomb repulsion U limit, the system is described by the KK model or molecular Mott insulator with two orbitals (anti-bonding d_{z^2} and bonding $d_{x^2-y^2}$) if all the anti-bonding states of $d_{x^2-y^2}$ are empty, and the system is described by self-doped molecular Mott insulator if the anti-bonding $d_{x^2-y^2}$ is slightly occupied. The latter may form a molecular doublon with the bonding $d_{x^2-y^2}$ orbital of

the same spin, which does not cost U , hence providing holes in the background of the Mott insulator. We argue that the low energy physics is given by the doped two orbital $t - J$ model (more precisely KK model) in a square lattice. Superconductivity arises from nearest neighbor orbital and spin coupling, whose pairing symmetry depends on the inter-orbital pairing strength. Our theory predicts more complex spin excitation in $\text{La}_3\text{Ni}_2\text{O}_7$ than in cuprates because of the two orbitals. Chemical hole doping, such as partial replacement of La by valence $2+$ ions (Ca or Sr) and interstitial oxygens, could introduce additional mobile holes hence good for superconductivity. For electron doping, the apical oxygen vacancies between bilayer Ni atoms destroy the molecular orbital, especially the anti-binding Fermi surface [48]. Therefore, the oxygen vacancies play a similar role as impurities on CuO_2 planes in cuprates and severely damage the superconductivity.

Acknowledgement. We acknowledge the support by the National Natural Science Foundation of China (Grant NSFC-12494590, No. NSFC-12174428), the Ministry of Science and Technology (Grant No. 2022YFA1403900), the Chinese Academy of Sciences Project for Young Scientists in Basic Research (2022Y5BR-048), the Innovation program for Quantum Science and Technology (Grant No. 2021ZD0302500), and Chinese Academy of Sciences under contract No. JZHKYPT-2021-08.

* jiangkun@iphy.ac.cn

† fuchun@ucas.ac.cn

- [1] B. Keimer, S. A. Kivelson, M. R. Norman, S. Uchida, and J. Zaanen, “From quantum matter to high-temperature superconductivity in copper oxides,” *Nature* **518**, 179–186 (2015).
- [2] Patrick A. Lee, Naoto Nagaosa, and Xiao-Gang Wen, “Doping a mott insulator: Physics of high-temperature superconductivity,” *Rev. Mod. Phys.* **78**, 17–85 (2006).
- [3] P W Anderson, P A Lee, M Randeria, T M Rice, N Trivedi, and F C Zhang, “The physics behind high-temperature superconducting cuprates: the ‘plain vanilla’ version of RVB,” *Journal of Physics: Condensed Matter* **16**, R755 (2004).
- [4] V. I. Anisimov, D. Bukhalov, and T. M. Rice, “Electronic structure of possible nickelate analogs to the cuprates,” *Phys. Rev. B* **59**, 7901–7906 (1999).
- [5] Danfeng Li, Kyuho Lee, Bai Yang Wang, Motoki Osada, Samuel Crossley, Hye Ryoung Lee, Yi Cui, Yasuyuki Hikita, and Harold Y. Hwang, “Superconductivity in an infinite-layer nickelate,” *Nature* **572**, 624–627 (2019).
- [6] Danfeng Li, Bai Yang Wang, Kyuho Lee, Shannon P. Harvey, Motoki Osada, Berit H. Goodge, Lena F. Kourkoutis, and Harold Y. Hwang, “Superconducting Dome in $\text{Nd}_{1-x}\text{Sr}_x\text{NiO}_2$ Infinite Layer Films,” *Phys. Rev. Lett.* **125**, 027001 (2020).
- [7] Motoki Osada, Bai Yang Wang, Kyuho Lee, Danfeng Li, and Harold Y. Hwang, “Phase diagram of infinite layer praseodymium nickelate $\text{Pr}_{1-x}\text{Sr}_x\text{NiO}_2$ thin films,” *Phys. Rev. Mater.* **4**, 121801 (2020).
- [8] Michael R. Norman, “Entering the Nickel Age of Superconductivity,” *Physics* **13**, 85 (2020).
- [9] Hualei Sun, Mengwu Huo, Xunwu Hu, Jingyuan Li, Zengjia Liu, Yifeng Han, Lingyun Tang, Zhongquan Mao, Pengtao Yang, Bosen Wang, Jinguang Cheng, Dao-Xin Yao, Guang-Ming Zhang, and Meng Wang, “Signatures of superconductivity near 80 K in a nickelate under high pressure,” *Nature* **621**, 493–498 (2023).
- [10] Zengjia Liu, Hualei Sun, Mengwu Huo, Xiaoyan Ma, Yi Ji, Enkui Yi, Lisi Li, Hui Liu, Jia Yu, Ziyou Zhang, Zhiqiang Chen, Feixiang Liang, Hongliang Dong, Hanjie Guo, Dingyong Zhong, Bing Shen, Shiliang Li, and Meng Wang, “Evidence for charge and spin density waves in single crystals of $\text{La}_3\text{Ni}_2\text{O}_7$ and $\text{La}_3\text{Ni}_2\text{O}_6$,” *Science China Physics, Mechanics & Astronomy* **66**, 217411 (2022).
- [11] Jun Hou, Peng-Tao Yang, Zi-Yi Liu, Jing-Yuan Li, Peng-Fei Shan, Liang Ma, Gang Wang, Ning-Ning Wang, Hai-Zhong Guo, Jian-Ping Sun, *et al.*, “Emergence of high-temperature superconducting phase in pressurized $\text{La}_3\text{Ni}_2\text{O}_7$ crystals,” *Chinese Physics Letters* **40**, 117302 (2023).
- [12] G. Wang, N. N. Wang, X. L. Shen, J. Hou, L. Ma, L. F. Shi, Z. A. Ren, Y. D. Gu, H. M. Ma, P. T. Yang, Z. Y. Liu, H. Z. Guo, J. P. Sun, G. M. Zhang, S. Calder, J.-Q. Yan, B. S. Wang, Y. Uwatoko, and J.-G. Cheng, “Pressure-Induced Superconductivity In Polycrystalline $\text{La}_3\text{Ni}_2\text{O}_{7-\delta}$,” *Phys. Rev. X* **14**, 011040 (2024).
- [13] Yanan Zhang, Dajun Su, Yanen Huang, Zhaoyang Shan, Hualei Sun, Mengwu Huo, Kaixin Ye, Jiawen Zhang, Zihan Yang, Yongkang Xu, Yi Su, Rui Li, Michael Smidman, Meng Wang, Lin Jiao, and Huiqiu Yuan, “High-temperature superconductivity with zero resistance and strange-metal behaviour in $\text{La}_3\text{Ni}_2\text{O}_{7-\delta}$,” *Nature Physics* **20**, 1269–1273 (2024).
- [14] Ningning Wang, Gang Wang, Xiaoling Shen, Jun Hou, Jun Luo, Xiaoping Ma, Huaixin Yang, Lifan Shi, Jie Dou, Jie Feng, Jie Yang, Yunqing Shi, Zhian Ren, Hanming Ma, Pengtao Yang, Ziyi Liu, Yue Liu, Hua Zhang, Xiaoli Dong, Yuxin Yang, Kun Jiang, Jiangping Hu, Shoko Nagasaki, Kentaro Kitagawa, Stuart Calder, Jiaqiang Yan, Jianping Sun, Bosen Wang, Rui Zhou, Yoshiya Uwatoko, and Jinguang Cheng, “Bulk high-temperature superconductivity in pressurized tetragonal $\text{La}_2\text{PrNi}_2\text{O}_7$,” *Nature* **634**, 579–584 (2024).
- [15] Zhihui Luo, Xunwu Hu, Meng Wang, Wéi Wú, and Dao-Xin Yao, “Bilayer Two-Orbital Model of $\text{La}_3\text{Ni}_2\text{O}_7$ under Pressure,” *Phys. Rev. Lett.* **131**, 126001 (2023).
- [16] Qing-Geng Yang, Da Wang, and Qiang-Hua Wang, “Possible s_{\pm} -wave superconductivity in $\text{La}_3\text{Ni}_2\text{O}_7$,” *Phys. Rev. B* **108**, L140505 (2023).
- [17] Yang Shen, Mingpu Qin, and Guang-Ming Zhang, “Effective Bi-Layer Model Hamiltonian and Density-Matrix Renormalization Group Study for the High- T_c Superconductivity in $\text{La}_3\text{Ni}_2\text{O}_7$ under High Pressure,” *Chinese Physics Letters* **40**, 127401 (2023).
- [18] Yang Zhang, Ling-Fang Lin, Adriana Moreo, and Elbio Dagotto, “Electronic structure, dimer physics, orbital-selective behavior, and magnetic tendencies in the bilayer nickelate superconductor $\text{La}_3\text{Ni}_2\text{O}_7$ under pressure,” *Phys. Rev. B* **108**, L180510 (2023).
- [19] Viktor Christiansson, Francesco Petocchi, and Philipp Werner, “Correlated Electronic Structure of $\text{La}_3\text{Ni}_2\text{O}_7$ under Pressure,” *Phys. Rev. Lett.* **131**, 206501 (2023).
- [20] Yi-feng Yang, Guang-Ming Zhang, and Fu-Chun Zhang, “Interlayer valence bonds and two-component theory for high- T_c superconductivity of $\text{La}_3\text{Ni}_2\text{O}_7$ under pressure,” *Phys. Rev. B* **108**, L201108 (2023).
- [21] Frank Lechermann, Jannik Gondolf, Steffen Bötzel, and Ilya M. Eremin, “Electronic correlations and superconducting instability in $\text{La}_3\text{Ni}_2\text{O}_7$ under high pressure,” *Phys. Rev. B* **108**, L201121 (2023).

- [22] Yu-Bo Liu, Jia-Wei Mei, Fei Ye, Wei-Qiang Chen, and Fan Yang, “ s^{\pm} -Wave Pairing and the Destructive Role of Apical-Oxygen Deficiencies in $\text{La}_3\text{Ni}_2\text{O}_7$ under Pressure,” *Phys. Rev. Lett.* **131**, 236002 (2023).
- [23] Xing-Zhou Qu, Dai-Wei Qu, Jialin Chen, Congjun Wu, Fan Yang, Wei Li, and Gang Su, “Bilayer t - J - J_{\perp} Model and Magnetically Mediated Pairing in the Pressurized Nickelate $\text{La}_3\text{Ni}_2\text{O}_7$,” *Phys. Rev. Lett.* **132**, 036502 (2024).
- [24] Kun Jiang, Ziqiang Wang, and Fu-Chun Zhang, “High-Temperature Superconductivity in $\text{La}_3\text{Ni}_2\text{O}_7$,” *Chinese Physics Letters* **41**, 017402 (2024).
- [25] Hirofumi Sakakibara, Naoya Kitamine, Masayuki Ochi, and Kazuhiko Kuroki, “Possible high T_c superconductivity in $\text{La}_3\text{Ni}_2\text{O}_7$ under high pressure through manifestation of a nearly half-filled bilayer hubbard model,” *Phys. Rev. Lett.* **132**, 106002 (2024).
- [26] Zhenfeng Ouyang, Jia-Ming Wang, Jing-Xuan Wang, Rong-Qiang He, Li Huang, and Zhong-Yi Lu, “Hund electronic correlation in $\text{La}_3\text{Ni}_2\text{O}_7$ under high pressure,” *Phys. Rev. B* **109**, 115114 (2024).
- [27] Yang Zhang, Ling-Fang Lin, Adriana Moreo, Thomas A. Maier, and Elbio Dagotto, “Structural phase transition, s_{\pm} -wave pairing, and magnetic stripe order in bilayered superconductor $\text{La}_3\text{Ni}_2\text{O}_7$ under pressure,” *Nature Communications* **15**, 2470 (2024).
- [28] Chen Lu, Zhiming Pan, Fan Yang, and Congjun Wu, “Interlayer-coupling-driven high-temperature superconductivity in $\text{La}_3\text{Ni}_2\text{O}_7$ under pressure,” *Phys. Rev. Lett.* **132**, 146002 (2024).
- [29] Zhen Fan, Jian-Feng Zhang, Bo Zhan, Dingshun Lv, Xing-Yu Jiang, Bruce Normand, and Tao Xiang, “Superconductivity in nickelate and cuprate superconductors with strong bilayer coupling,” *Phys. Rev. B* **110**, 024514 (2024).
- [30] Siheon Ryee, Niklas Witt, and Tim O. Wehling, “Quenched Pair Breaking by Interlayer Correlations as a Key to Superconductivity in $\text{La}_3\text{Ni}_2\text{O}_7$,” *Phys. Rev. Lett.* **133**, 096002 (2024).
- [31] Yuhao Gu, Congcong Le, Zhesen Yang, Xianxin Wu, and Jiangping Hu, “Effective model and pairing tendency in bilayer Ni-based superconductor $\text{La}_3\text{Ni}_2\text{O}_7$,” *arXiv e-prints*, arXiv:2306.07275 (2023).
- [32] Nejat Bulut, Douglas J. Scalapino, and Richard T. Scalettar, “Nodeless d-wave pairing in a two-layer hubbard model,” *Phys. Rev. B* **45**, 5577–5584 (1992).
- [33] R. E. Hetzel, W. von der Linden, and W. Hanke, “Pairing correlations in a two-layer hubbard model,” *Phys. Rev. B* **50**, 4159–4162 (1994).
- [34] Richard T. Scalettar, Joel W. Cannon, Douglas J. Scalapino, and Robert L. Sugar, “Magnetic and pairing correlations in coupled hubbard planes,” *Phys. Rev. B* **50**, 13419–13427 (1994).
- [35] Raimundo R. dos Santos, “Magnetism and pairing in hubbard bilayers,” *Phys. Rev. B* **51**, 15540–15546 (1995).
- [36] S. S. Kancharla and S. Okamoto, “Band insulator to mott insulator transition in a bilayer hubbard model,” *Phys. Rev. B* **75**, 193103 (2007).
- [37] K. Bouadim, G. G. Batrouni, F. Hébert, and R. T. Scalettar, “Magnetic and transport properties of a coupled hubbard bilayer with electron and hole doping,” *Phys. Rev. B* **77**, 144527 (2008).
- [38] Nicola Lanatà, Paolo Barone, and Michele Fabrizio, “Superconductivity in the doped bilayer hubbard model,” *Phys. Rev. B* **80**, 224524 (2009).
- [39] T. A. Maier and D. J. Scalapino, “Pair structure and the pairing interaction in a bilayer hubbard model for unconventional superconductivity,” *Phys. Rev. B* **84**, 180513 (2011).
- [40] F. C. Zhang and T. M. Rice, “Effective Hamiltonian for the superconducting Cu oxides,” *Phys. Rev. B* **37**, 3759–3761 (1988).
- [41] F C Zhang, C Gros, T M Rice, and H Shiba, “A renormalised hamiltonian approach to a resonant valence bond wavefunction,” *Superconductor Science and Technology* **1**, 36 (1988).
- [42] Yuxin Wang, Kun Jiang, Ziqiang Wang, Fu-Chun Zhang, and Jiangping Hu, “Electronic and magnetic structures of bilayer $\text{La}_3\text{Ni}_2\text{O}_7$ at ambient pressure,” *Phys. Rev. B* **110**, 205122 (2024).
- [43] K. I. Kugel’ and D. I. Khomskii, “Crystal structure and magnetic properties of substances with orbital degeneracy,” *Soviet Journal of Experimental and Theoretical Physics* **37**, 725 (1973).
- [44] C. Castellani, C. R. Natoli, and J. Ranninger, “Magnetic structure of V_2O_3 in the insulating phase,” *Phys. Rev. B* **18**, 4945–4966 (1978).
- [45] Daniel I. Khomskii, *Transition Metal Compounds* (Cambridge University Press, 2014).
- [46] A. Rüegg, M. Indergand, S. Pilgram, and M. Sigrist, “Slave-boson mean-field theory of the mott transition in the two-band hubbard model,” *The European Physical Journal B - Condensed Matter and Complex Systems* **48**, 55–64 (2005).
- [47] Frank Lechermann, Antoine Georges, Gabriel Kotliar, and Olivier Parcollet, “Rotationally invariant slave-boson formalism and momentum dependence of the quasiparticle weight,” *Phys. Rev. B* **76**, 155102 (2007).
- [48] Yuxin Wang, Yi Zhang, and Kun Jiang, “The electronic structure and disorder effect of $\text{La}_3\text{Ni}_2\text{O}_7$ superconductor,” (2024), arXiv:2412.20465 [cond-mat.supr-con].

The sum over ij covers all the nearest neighbor bonds of site i and the vector connecting ij is denoted as $\mathbf{r}_{ij} = \mathbf{r}_i - \mathbf{r}_j$. For the two antisymmetric orbitals:

$$\begin{aligned} \epsilon_{\mathbf{k}}^{\alpha\alpha'} = & - \sum_{ij} g_t^{\alpha\alpha'} t_{ij}^{\alpha\alpha'} e^{-i\mathbf{k}\cdot\mathbf{r}_{ij}} - \frac{1}{2U} \sum_{\beta} \sum_{ij} \left(t_{ij}^{\beta\alpha'} t_{ij}^{\alpha\alpha'} \chi_{ij}^{\beta\alpha'} - t_{ij}^{\beta\bar{\alpha}'} t_{ij}^{\alpha\bar{\alpha}'} \chi_{ij}^{\beta\alpha'} + 2t_{ij}^{\beta\bar{\alpha}'} t_{ij}^{\alpha\alpha'} \chi_{ij}^{\beta\bar{\alpha}'} \right) e^{-i\mathbf{k}\cdot\mathbf{r}_{ij}} \\ & - \frac{1}{2U} \sum_{\beta} \sum_{ij} \left(t_{ij}^{\beta\alpha} t_{ij}^{\alpha'\alpha} \chi_{ij}^{\beta\alpha} - t_{ij}^{\beta\bar{\alpha}} t_{ij}^{\alpha'\bar{\alpha}} \chi_{ij}^{\beta\alpha} + 2t_{ij}^{\beta\bar{\alpha}} t_{ij}^{\alpha'\alpha} \chi_{ij}^{\beta\bar{\alpha}} \right) e^{i\mathbf{k}\cdot\mathbf{r}_{ij}}. \end{aligned} \quad (\text{S9})$$

For pairings:

$$\begin{aligned} \Delta_{\mathbf{k}}^{\alpha\alpha'} = & - \frac{1}{2U} \sum_{\beta} \sum_{ij} \left(2t_{ij}^{\beta\alpha'} t_{ij}^{\alpha\alpha'} \Delta_{ij}^{\beta\alpha'} + t_{ij}^{\beta\alpha'} t_{ij}^{\alpha\bar{\alpha}'} \Delta_{ij}^{\beta\bar{\alpha}'} + t_{ij}^{\beta\bar{\alpha}'} t_{ij}^{\alpha\alpha'} \Delta_{ij}^{\beta\alpha'} \right) e^{-i\mathbf{k}\cdot\mathbf{r}_{ij}} \\ & - \frac{1}{2U} \sum_{\beta} \sum_{ij} \left(2t_{ij}^{\beta\alpha} t_{ij}^{\alpha'\alpha} \Delta_{ij}^{\beta\alpha} + t_{ij}^{\beta\alpha} t_{ij}^{\alpha'\bar{\alpha}} \Delta_{ij}^{\beta\bar{\alpha}} + t_{ij}^{\beta\bar{\alpha}} t_{ij}^{\alpha'\alpha} \Delta_{ij}^{\beta\alpha} \right) e^{i\mathbf{k}\cdot\mathbf{r}_{ij}}. \end{aligned} \quad (\text{S10})$$

Here the orbital index $\alpha\alpha'\beta$ can take either x or z , referring to the two antisymmetric orbitals $|x, -\rangle$ and $|z, -\rangle$. The inverse index $\bar{\alpha}$ refers to the other orbital with the different index from α .

The Hamiltonian can be diagonalized by a unitary transformation $U^{\mathbf{k}}$ to get the Bogoliubov-de-Gennes quasiparticle dispersion $E_{n\mathbf{k}}$ and the corresponding quasi-particles $d_{n\mathbf{k}}$:

$$\Lambda_{\mathbf{k}} = U^{\mathbf{k}\dagger} H_{MF}^{\mathbf{k}} U^{\mathbf{k}}, \quad (\text{S11})$$

where $\Lambda_{\mathbf{k}}$ is the diagonal matrix of the quasiparticle energy eigenvalue $E_{n\mathbf{k}}$. The self-consistent equations can be written in terms of the matrix elements of $U^{\mathbf{k}}$, denoted as $u_{in}^{\mathbf{k}}$. For pairing mean fields:

$$\begin{aligned} \Delta_{ij}^{xx} = & \langle c_{ix\uparrow}^{\dagger} c_{jx\downarrow}^{\dagger} \rangle - \langle c_{ix\downarrow}^{\dagger} c_{jx\uparrow}^{\dagger} \rangle = \frac{1}{N} \sum_{\mathbf{k}} \left[e^{-i\mathbf{k}\cdot\mathbf{r}_{ij}} \sum_n u_{2n}^{\mathbf{k}*} u_{5n}^{\mathbf{k}} n_F(E_{n\mathbf{k}}) + e^{i\mathbf{k}\cdot\mathbf{r}_{ij}} \sum_n u_{2n}^{\mathbf{k}} u_{5n}^{\mathbf{k}*} n_F(E_{n\mathbf{k}}) \right], \\ \Delta_{ij}^{xz} = & \langle c_{ix\uparrow}^{\dagger} c_{jz\downarrow}^{\dagger} \rangle - \langle c_{ix\downarrow}^{\dagger} c_{jz\uparrow}^{\dagger} \rangle = \frac{1}{N} \sum_{\mathbf{k}} \left[e^{-i\mathbf{k}\cdot\mathbf{r}_{ij}} \sum_n u_{2n}^{\mathbf{k}*} u_{6n}^{\mathbf{k}} n_F(E_{n\mathbf{k}}) + e^{i\mathbf{k}\cdot\mathbf{r}_{ij}} \sum_n u_{3n}^{\mathbf{k}*} u_{5n}^{\mathbf{k}} n_F(E_{n\mathbf{k}}) \right] = \Delta_{ij}^{zx}, \\ \Delta_{ij}^{zz} = & \langle c_{iz\uparrow}^{\dagger} c_{jz\downarrow}^{\dagger} \rangle - \langle c_{iz\downarrow}^{\dagger} c_{jz\uparrow}^{\dagger} \rangle = \frac{1}{N} \sum_{\mathbf{k}} \left[e^{-i\mathbf{k}\cdot\mathbf{r}_{ij}} \sum_n u_{3n}^{\mathbf{k}*} u_{6n}^{\mathbf{k}} n_F(E_{n\mathbf{k}}) + e^{i\mathbf{k}\cdot\mathbf{r}_{ij}} \sum_n u_{3n}^{\mathbf{k}} u_{6n}^{\mathbf{k}*} n_F(E_{n\mathbf{k}}) \right]. \end{aligned}$$

Here $n_F(E_{n\mathbf{k}})$ denotes the Fermi-Dirac distribution of the quasiparticle with energy $E_{n\mathbf{k}}$. The last equality of the second line comes from the ansatz that the pairing is an even function of the orbital index. For hopping mean fields:

$$\begin{aligned} \chi_{ij}^{xx} = & \langle c_{ix\uparrow}^{\dagger} c_{jx\uparrow} \rangle + \langle c_{ix\downarrow}^{\dagger} c_{jx\downarrow} \rangle = \frac{1}{N} \sum_{\mathbf{k}} \left[e^{-i\mathbf{k}\cdot\mathbf{r}_{ij}} \sum_n u_{2n}^{\mathbf{k}*} u_{2n}^{\mathbf{k}} n_F(E_{n\mathbf{k}}) + e^{i\mathbf{k}\cdot\mathbf{r}_{ij}} \sum_n u_{5n}^{\mathbf{k}} u_{5n}^{\mathbf{k}*} (1 - n_F(E_{n\mathbf{k}})) \right], \\ \chi_{ij}^{xz} = & \langle c_{ix\uparrow}^{\dagger} c_{jz\uparrow} \rangle + \langle c_{ix\downarrow}^{\dagger} c_{jz\downarrow} \rangle = \frac{1}{N} \sum_{\mathbf{k}} \left[e^{-i\mathbf{k}\cdot\mathbf{r}_{ij}} \sum_n u_{2n}^{\mathbf{k}*} u_{3n}^{\mathbf{k}} n_F(E_{n\mathbf{k}}) + e^{i\mathbf{k}\cdot\mathbf{r}_{ij}} \sum_n u_{5n}^{\mathbf{k}} u_{6n}^{\mathbf{k}*} (1 - n_F(E_{n\mathbf{k}})) \right], \\ \chi_{ij}^{zz} = & \langle c_{iz\uparrow}^{\dagger} c_{jz\uparrow} \rangle + \langle c_{iz\downarrow}^{\dagger} c_{jz\downarrow} \rangle = \frac{1}{N} \sum_{\mathbf{k}} \left[e^{-i\mathbf{k}\cdot\mathbf{r}_{ij}} \sum_n u_{3n}^{\mathbf{k}*} u_{3n}^{\mathbf{k}} n_F(E_{n\mathbf{k}}) + e^{i\mathbf{k}\cdot\mathbf{r}_{ij}} \sum_n u_{6n}^{\mathbf{k}} u_{6n}^{\mathbf{k}*} (1 - n_F(E_{n\mathbf{k}})) \right]. \end{aligned}$$

And the particle number can be calculated according to:

$$\begin{aligned} n_{x+} = & \langle f_{ix\uparrow}^{\dagger} f_{ix\uparrow} \rangle + \langle f_{ix\downarrow}^{\dagger} f_{ix\downarrow} \rangle = \frac{1}{N} \sum_{n\mathbf{k}} \left[u_{1n}^{\mathbf{k}*} u_{1n}^{\mathbf{k}} n_F(E_{n\mathbf{k}}) + u_{4n}^{\mathbf{k}} u_{4n}^{\mathbf{k}*} (1 - n_F(E_{n\mathbf{k}})) \right], \\ n_{x-} = & \langle c_{ix\uparrow}^{\dagger} c_{ix\uparrow} \rangle + \langle c_{ix\downarrow}^{\dagger} c_{ix\downarrow} \rangle = \frac{1}{N} \sum_{n\mathbf{k}} \left[u_{2n}^{\mathbf{k}*} u_{2n}^{\mathbf{k}} n_F(E_{n\mathbf{k}}) + u_{5n}^{\mathbf{k}} u_{5n}^{\mathbf{k}*} (1 - n_F(E_{n\mathbf{k}})) \right], \\ n_{z-} = & \langle c_{iz\uparrow}^{\dagger} c_{iz\uparrow} \rangle + \langle c_{iz\downarrow}^{\dagger} c_{iz\downarrow} \rangle = \frac{1}{N} \sum_{n\mathbf{k}} \left[u_{3n}^{\mathbf{k}*} u_{3n}^{\mathbf{k}} n_F(E_{n\mathbf{k}}) + u_{6n}^{\mathbf{k}} u_{6n}^{\mathbf{k}*} (1 - n_F(E_{n\mathbf{k}})) \right]. \end{aligned}$$

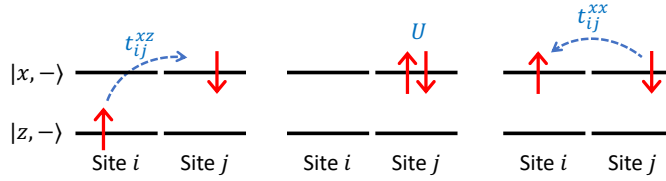


FIG. S1. Virtual hopping process corresponding to the interaction term $c_{ix\uparrow}^\dagger c_{jx\downarrow}^\dagger c_{jz\downarrow} c_{iz\uparrow}$, leading to the hybrid pairing interaction of the form $\Delta_{xx}^\dagger \Delta_{xz}$ with interaction strength $\propto t_{ij}^{xz} t_{ij}^{xx} / U$.

In calculations, the parameters are chosen as follows. The Hubbard interaction $U = 6$ and the in-plane nearest neighbor hoppings are given by $t^{xx} = 1$, $t^{zz} = 0.2$ according to [27] for the case of $\text{La}_3\text{Ni}_2\text{O}_7$. The interorbital hoppings $t^{xz} = 0.1$ and $t^{zx} = 0.8$ are considered. Moreover, the calculations are performed with varying number of self-doped holes n_h , which corresponds to varying the molecular energy splitting ϵ_{x+} . The total electron number is fixed by the chemical potential μ to yield $\langle n \rangle = \langle n_h \rangle + \langle n_{x-} \rangle + \langle n_{z-} \rangle = 1$, namely no external holes.

pairing interaction from the two-orbital process

The pairing part of the Hamiltonian takes the form:

$$H_{\text{pairing}} = \sum_{\langle ij \rangle} \sum_{\alpha\alpha'\beta} \left[-\frac{t_{ij}^{\alpha\beta} t_{ij}^{\alpha'\beta}}{2U} (2\Delta_{ij}^{\alpha'\beta,\dagger} \Delta_{ij}^{\alpha\beta} + \Delta_{ij}^{\alpha'\beta,\dagger} \Delta_{ij}^{\alpha\beta}) - \frac{t_{ij}^{\alpha\beta} t_{ij}^{\alpha'\beta}}{2U} \Delta_{ij}^{\alpha'\beta,\dagger} \Delta_{ij}^{\alpha\beta} \right]. \quad (\text{S12})$$

By further considering the orbital indices, the pairing part can be divided into the intra-orbital, inter-orbital as well as hybrid channels (sum over α is implied):

$$H_{\text{pairing}}^{\text{intra-orbital}} = -\frac{t_{ij}^{\alpha\alpha} t_{ij}^{\alpha\alpha}}{U} \Delta_{ij}^{\alpha\alpha,\dagger} \Delta_{ij}^{\alpha\alpha} - \frac{t_{ij}^{\alpha\bar{\alpha}} t_{ij}^{\alpha\bar{\alpha}}}{2U} \Delta_{ij}^{\alpha\alpha,\dagger} \Delta_{ij}^{\alpha\alpha} - \frac{t_{ij}^{\bar{\alpha}\alpha} t_{ij}^{\bar{\alpha}\alpha}}{2U} \Delta_{ij}^{\alpha\alpha,\dagger} \Delta_{ij}^{\bar{\alpha}\bar{\alpha}}, \quad (\text{S13})$$

$$H_{\text{pairing}}^{\text{inter-orbital}} = -\frac{t_{ij}^{\alpha\bar{\alpha}} t_{ij}^{\alpha\bar{\alpha}}}{U} \Delta_{ij}^{\alpha\bar{\alpha},\dagger} \Delta_{ij}^{\alpha\bar{\alpha}} - \frac{t_{ij}^{\alpha\alpha} t_{ij}^{\alpha\alpha}}{2U} \Delta_{ij}^{\alpha\bar{\alpha},\dagger} \Delta_{ij}^{\alpha\bar{\alpha}} - \frac{t_{ij}^{\bar{\alpha}\alpha} t_{ij}^{\bar{\alpha}\alpha}}{2U} \Delta_{ij}^{\alpha\bar{\alpha},\dagger} \Delta_{ij}^{\alpha\bar{\alpha}}, \quad (\text{S14})$$

$$H_{\text{pairing}}^{\text{hybrid}} = -\frac{t_{ij}^{\alpha\alpha} t_{ij}^{\bar{\alpha}\alpha}}{U} \Delta_{ij}^{\bar{\alpha}\alpha,\dagger} \Delta_{ij}^{\alpha\alpha} - \frac{t_{ij}^{\alpha\alpha} t_{ij}^{\bar{\alpha}\alpha}}{2U} \Delta_{ij}^{\bar{\alpha}\bar{\alpha},\dagger} \Delta_{ij}^{\alpha\bar{\alpha}} - \frac{t_{ij}^{\bar{\alpha}\alpha} t_{ij}^{\alpha\alpha}}{2U} \Delta_{ij}^{\bar{\alpha}\bar{\alpha},\dagger} \Delta_{ij}^{\alpha\alpha} + \text{h.c.} \quad (\text{S15})$$

The last equation is unique to the considered two orbital interactions. Taking the first term in the last line, $-\frac{t_{ij}^{\alpha\alpha} t_{ij}^{\bar{\alpha}\alpha}}{U} \Delta_{ij}^{\bar{\alpha}\alpha,\dagger} \Delta_{ij}^{\alpha\alpha}$, and set $\alpha = x$, $\bar{\alpha} = z$ as an example, the virtual process giving this term can be depicted in Fig.S1.